



HAL
open science

Dynamic and rheological properties of classic and macromolecular surfactant at the supercritical CO₂-H₂O interface

Frédéric Tewes, Frank Boury

► **To cite this version:**

Frédéric Tewes, Frank Boury. Dynamic and rheological properties of classic and macromolecular surfactant at the supercritical CO₂-H₂O interface. *Journal of Supercritical Fluids*, 2006, 37 (3), pp.375-383. 10.1016/j.supflu.2006.02.005 . inserm-00264738

HAL Id: inserm-00264738

<https://inserm.hal.science/inserm-00264738>

Submitted on 17 Mar 2008

HAL is a multi-disciplinary open access archive for the deposit and dissemination of scientific research documents, whether they are published or not. The documents may come from teaching and research institutions in France or abroad, or from public or private research centers.

L'archive ouverte pluridisciplinaire **HAL**, est destinée au dépôt et à la diffusion de documents scientifiques de niveau recherche, publiés ou non, émanant des établissements d'enseignement et de recherche français ou étrangers, des laboratoires publics ou privés.

Dynamic and rheological properties of classic and macromolecular surfactant at the supercritical CO₂–H₂O interface

Frederic Tewes, Frank Boury*

*Inserm U646, Ingénierie de la Vectorisation Particulaire, Université d'Angers, Bat. IBT,
10 rue A. Boquel, Angers F-49100, France*

Received 15 June 2005; received in revised form 20 February 2006; accepted 20 February 2006

Abstract

For the first time, rheological and dynamical properties of various interfacial layers separating an aqueous phase and a carbon dioxide phase under supercritical conditions have been measured by means of a drop tensiometer, applying either sinusoidal or ramp interfacial area perturbation. Those approaches have been largely developed on liquid–air and liquid–liquid interface but very few studies were performed in pressurized conditions [F. Tewes, F. Boury, Formation and rheological properties of the supercritical CO₂–water pure interface, *J. Phys. Chem. B* 109 (2005) 3990–3997; F. Tewes, F. Boury, Effect of H₂O–CO₂ organization on ovalbumin adsorption at the supercritical CO₂–water interface, *J. Phys. Chem. B* 109 (2005) 1874–1881].

For small surfactants, such as Tween® molecules, same results for equilibrium elasticity (E_e) values were obtained whatever the perturbation mode. However, non-equilibrium elasticity values (E_{ne}) were in some cases significantly influenced by the kind of perturbation. Rheological measurements evidenced the effect of the size of the alkyl tail upon the rheological properties of the interface. In particular, an alkyl chain composed of 16 carbon atoms facilitated the formation of a mixed interface constituted from Tween® molecules and a network of structured H₂O–CO₂ molecules.

Polymeric molecules like human serum albumin (HSA), produced interfacial films with an important elasticity. For these systems, E_e and E_{ne} varied with CO₂ pressure and with the type of protein.

© 2006 Elsevier B.V. All rights reserved.

Keywords: Interfacial tension; Supercritical; Protein; Surfactants; Adsorption; Dilational rheology

1. Introduction

The interest in the use of carbon dioxide into supercritical conditions (ScCO₂) increases for a lot of application such as medium reaction [3], foaming agent or non-miscible phase for emulsion and microemulsion formulation [4]. This can be attributed to the peculiar physical properties of supercritical fluids, allowing easily and in continuous way the tuning of their density and their solvent power. Moreover, the use of CO₂ answers to the need of the substituting toxic and environmentally bad organic solvent in the industrial processes.

In the last years, many studies deal with the formation of W/C and C/W microemulsion [4–6] and emulsion [7]. The first experiments were feasibility studies, with the search

of very CO₂-soluble surfactant (i.e. with fluoroalkyl, fluoroether or silicone tails). Almost studies were based on phase behavior, droplet size determination, solubilization efficiency, conductivity and interfacial tension measurements [7–11]. However, a small number of studies have measured γ between H₂O and CO₂ in presence of surfactant [2,7,11–15] and few of these studies included interfacial rheology measurement [2].

The dispersed droplets in an emulsion are in constant motion and there are frequent collisions between them in absence of steric and/or electrical barrier. These collisions lead to droplets aggregation and, if the interfacial wall is broken, to an irreversible coalescence of the droplets. In C/W emulsion, this kind of barrier can be easily created, as this is done in O/W emulsion. Unfortunately, in W/C emulsion, it is very difficult to obtain such barrier without the use of surfactants containing fluoroalkyl or fluoroether tails [16]. As a matter of fact, few polymers are soluble enough in CO₂, except fluoropolymers, siloxane and

* Corresponding author. Tel.: +33 2 41 73 58 48; fax: +33 2 41 73 58 03.
E-mail address: frank.boury@univ-angers.fr (F. Boury).

polycarbonate to create a steric barrier. Furthermore, CO₂ has a low dielectric constant, which renders difficult the creation of an electrostatic barrier.

Consequently, in a CO₂ medium, without the use of very CO₂-phile surfactants often containing a fluorinated-tail, aqueous droplets frequently interact and coalesce when the interfacial wall is broken. Indeed, the mechanical strength of the interfacial film is therefore one of the prime factors determining W/C emulsion stability.

The interfacial elasticity related to the organization of the surfactant layer is such that any applied strain that tends towards local thinning or stretching of the interface is counterbalanced by opposite forces that restore the initial conditions. This elasticity can be separated in two elements: an equilibrium elasticity (E_e), which describes surfactant interactions in the interfacial layer (i.e. lateral interaction). A non-equilibrium elasticity (E_{ne}) that can be related to the interactions of surfactant with adjacent phases (i.e. desorption and reorganization of the interface), associated with a relaxation time τ representing the necessary time for the interface to reach a new equilibrium energetic state after the perturbation.

We have previously investigated the formation of pure water–CO₂ interface by means of a drop tensiometer [1,17]. We have described it as a two-step phenomenon. Firstly, the CO₂ molecules quickly adsorb onto the water surface for equilibrating their chemical potential between the bulk CO₂ and the water surface. This physisorption leads to the interaction of one CO₂ molecule with one H₂O molecules. Secondly, CO₂ molecules diffuse into the water subsurface and then modify the water organization. This reorganization of the water molecules creates a network of H₂O–CO₂ clusters to form an interphase and leads to a decrease of γ until an equilibrium state. These H₂O–CO₂ clusters are formed at temperature upper (20–40 °C) to the one usually described as the limit (10 °C) for the formation of the crystalline structure called clathrate hydrate [18–20].

Elasticity measurements and macroscopic visualization suggest that the growing of clusters is driven by assembly of many small blocks and accelerates with the CO₂ pressure. Their interfacial concentration and their size increase with time until the saturation of the interface.

A fundamental understanding of interfacial surfactant adsorption and the rheological properties of H₂O–CO₂ interface is then useful for designing surfactants that stabilize efficiently W/C emulsions.

This must be performed by first understanding the rheological comportment of the pure H₂O–CO₂ interface and then by the measurement of interfacial properties in presence of different surfactants.

We described in this paper the measurement of rheological parameters of H₂O–CO₂ interface in presence of small or macromolecular adsorbed molecules. We compared two kinds of rheological approach consisting either of a sinusoidal or a ramp interfacial area perturbation.

2. Materials and methods

2.1. Pendant drop tensiometer

The drop tensiometer (Tracker, IT Concept, France) allows the determination of the interfacial tension by analyzing the axial symmetric shape (Laplacian profile) of the pendant drop (aqueous phase) in CO₂. The apparatus consists in a view cell under CO₂ atmosphere, a light source, a CCD camera, a computer, a syringe (Exmire microsyringe MS*GLL100, ITO corporation, Japan) and a motor as described by Tewes and Boury [1,2,17]. The syringe was filled with pure water and coupled to the view cell. Then, the view cell was pressurized with pure CO₂ until reaching the desired temperature (40 °C) and pressure. After that, the system is left during 24 h for equilibrating the water phase with the CO₂ phase. Pendant drops whose area is controlled during all the time of experience by the motor were formed at the end of a stainless steel needles (needles 20 G, popper, USA), having an inside diameter of 1 mm and connected to the syringe.

2.2. Rheological measurements

A rheological experiment is performed by applying a controlled perturbation to the interface in order to simultaneously follow the related interfacial pressure variations, $\Delta\pi = \gamma(t) - \gamma_i$, with γ_i is the interfacial tension before the perturbation and $\gamma(t)$ the interfacial tension during or after the perturbation. In this study, the viscoelastic response of an interfacial film to a dilatational mechanical strain (ramp or sinusoidal) in the time scale of 1–10³ s is studied by means of two experimental approaches.

2.2.1. Ramp type perturbation approach

The first approach consists to realize two types of continuous and monotonic compression of the equilibrated interfacial layer

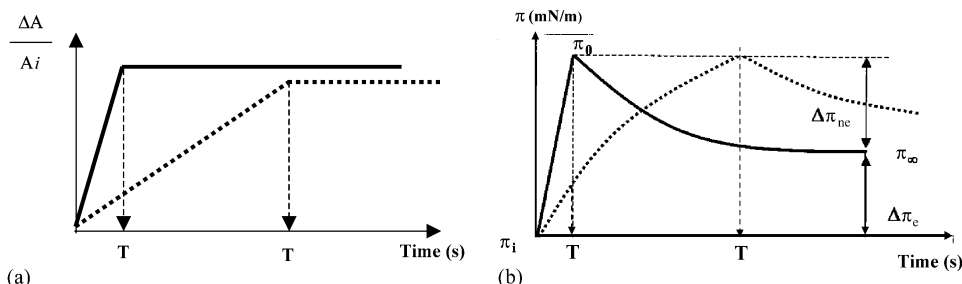


Fig. 1. Relative area (a) and interfacial pressure change $\Delta\pi$ (b) occurring during the time T of compression (bold line: fast compression; dashed line: slow compression).

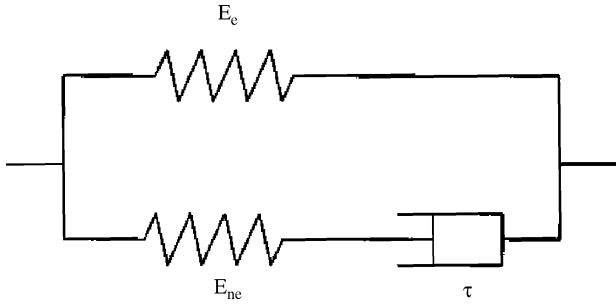


Fig. 2. Generalized Maxwell mechanical model.

on a pendant drop: a slow compression (dashed line) and fast compression (bold line) (Fig. 1a). Simultaneously, we record the variation of $\Delta\pi$ during the slow compression (dashed line) or after the fast compression to measure the relaxation of the interface (bold line) (Fig. 1b).

In this case, a convenient theoretical model (generalized Maxwell) (Fig. 2), corresponding to a viscoelastic body, has been developed and applied to many kinds of interfacial systems (phospholipids or polymers) [21–24].

In order to describe $\Delta\pi$ (i.e. resulting stress; Fig. 1b), during the time T of the compression performed at a constant velocity U_b , we supposed that at any one moment it can be written as a sum of equilibrium $\Delta\pi_e$ and non-equilibrium $\Delta\pi_{ne}$ contributions of the stresses:

$$\Delta\pi = \Delta\pi_e + \Delta\pi_{ne} \quad (1)$$

The equilibrium part of the resulting stress $\Delta\pi_e$ depends on the equilibrium interface dilatational elasticity E_e :

$$\Delta\pi_e = E_e \frac{U_b t}{A_i} \quad (2)$$

where A_i is the initial interfacial area before the mechanical strain:

$$\frac{U_b t}{A_i} \equiv \frac{\Delta A}{A_i} \quad (3)$$

This elastic behavior is represented by the upper branch of the mechanical model in Fig. 2. The non-equilibrium part of the resulting stress $\Delta\pi_{ne}$ is correlated to the accumulation of elastic energy during the compression. Dissipation of this accumulated energy occurs during compression as well as relaxation and can be interpreted as a molecular reorganization in the monolayer (i.e. desorption). This viscoelastic behavior can be described using the following equation:

$$\frac{d\Delta\pi_{ne}}{dt} + \frac{\Delta\pi_{ne}}{\tau} = E_{ne} \frac{U_b}{A_i} \quad (4)$$

where E_{ne} is the non-equilibrium interface dilatational elasticity and τ is the specific time of relaxation. The viscoelastic behavior is represented by the lower branch of the mechanical model in Fig. 2. If the initial conditions are $\Delta\pi_{ne} = 0$ at $t = 0$, so $\Delta\pi_{ne}$ can be written as:

$$\Delta\pi_{ne} = \frac{E_{ne} U_b t}{A_i} (1 - e^{-t/\tau}) \quad (5)$$

The two branches of the mechanical model are coupled in parallel according to Eq. (1) corresponding to the additivity of stresses; we obtained the following equation to describe the viscoelastic behavior of the monolayer:

$$\frac{\Delta\pi}{U_b t} A_i = E_e + E_{ne} \frac{\tau}{t} (1 - e^{-t/\tau}) \quad (6)$$

Using the experimental values found for $\Delta\pi(t)$ and with Eq. (6), it is possible to determine the non-equilibrium part (E_{ne}) and the equilibrium part (E_e) of the dilatational elasticity. The specific time of relaxation τ could be easily determined from experiments where the time of compression T was much smaller than the characteristic time of the relaxation process τ (fast compression).

For the determination of E_e , E_{ne} , and τ , one has to successively perform the following experiments:

- Fast compression ($d/dt \Delta A(t)/A_i = U/A_i$ typically higher than 0.005 s^{-1} , with $\Delta\pi_{\max}$ typically lower than 2 mN/m) in order to determine precisely the relaxation time τ . Subsequently, this characteristic time of relaxation is determined by fitting the γ relaxation curves by an exponential equation: $\gamma = \gamma_{\infty} + A e^{-t/\tau}$.
- Slow ($d/dt \Delta A(t)/A_i = U/A_i$ typically lower than 0.003 s^{-1}) monolayer compression (with $\Delta\pi_{\max} < 2 \text{ mN/m}$) in order to determine E_e and E_{ne} using the value of τ in Eq. (6).

2.2.2. Sinusoidal perturbation approach

In the second approach, a sinusoidal interfacial area deformation is applied at several frequencies in order to follow the γ response. Relative area variation versus time and interfacial pressure variation versus time are considered, respectively, as the input and the output of the interfacial system, from which it is possible to evaluate a transfer function (complex function) often called complex elasticity modulus E . The real part of this function characterizes conservative monolayer compartment. The imaginary part characterizes a dissipative monolayer compartment [21].

For each pulsation ω ($\omega = 2\pi f$ where f is the frequency of the oscillations), and at every time t , an adequate harmonic analysis of these two signals allows the calculation of a complex transfer function (or complex elasticity) given by:

$$\bar{G}(\omega) = \bar{E}(\omega) = \bar{A} \frac{d\pi}{dA} \quad (7)$$

We have verified that this complex function is independent of time when the interfacial tension γ has reached its equilibrium value. This transfer function can be transformed in the following expression:

$$\bar{G}(\omega) = G'(\omega) + iG''(\omega) \quad (8)$$

where $G'(\omega)$ and $G''(\omega)$ correspond, respectively, to the real part and the imaginary part of the transfer function. Therefore, the graphs $G'(\omega)$ and $G''(\omega)$ are characteristic of the rheological compartment of the interfacial layer. The dephasing angle φ is

also given by:

$$\operatorname{tg}(\varphi) = \frac{G'(\omega)}{G''(\omega)} \quad (9)$$

Considering that the interface follows a generalized Maxwell mechanical model previously described (Fig. 2), the conservative part of the transfer function ($G'(\omega)$) is theoretically represented by the following equations:

$$G'(\omega) = E_c + E_{ne} \frac{\omega^2 \tau^2}{1 + \omega^2 \tau^2} \quad (10)$$

Similarly, the imaginary part of the transfer function is written as:

$$G''(\omega) = E_{ne} \tau \frac{1}{1 + \omega^2 \tau^2} \quad (11)$$

The physical constants E_c , E_{ne} , and τ are extrapolated considering:

$$\lim_{\omega \rightarrow 0} G'(\omega) = E_c \quad (12)$$

$$\lim_{\omega \rightarrow +\infty} G'(\omega) = E_c + E_{ne} \quad (13)$$

$$\lim_{\omega \rightarrow 0} \frac{G''(\omega)}{\omega} = E_{ne} \tau \quad (14)$$

3. Results and discussion

We studied the behavior of the H₂O/pressurized CO₂ interface in presence of various kinds of Tween[®] molecules (Tween 20, 40, 60 and 80 (Fig. 3)) adsorbed from the aqueous phase. These Tween[®] molecules have the same hydrophilic part, composed of a sorbitan linked to three polyoxyethylene chains. However, their CO₂-philic part, composed of an alkyl chain, increase with their identification number from a dodecane chain (Tween[®] 20) to an octadecane chain (Tween[®] 80). By changing the CO₂-philic part of the molecule, and keeping constant the hydrophilic one, we can evaluate the effect of the CO₂-philic part on the interfacial tension and interfacial rheological properties of the adsorbed Tween[®] monolayer.

In this goal, we always performed the experiments at the same bulk concentration (0.075 wt.% in water), i.e. higher than the critical micellar concentration of Tween[®] in water at room conditions. At this concentration, the Tween[®] molecules were at their maximal interfacial compaction state, considering a Gibbs monolayer.

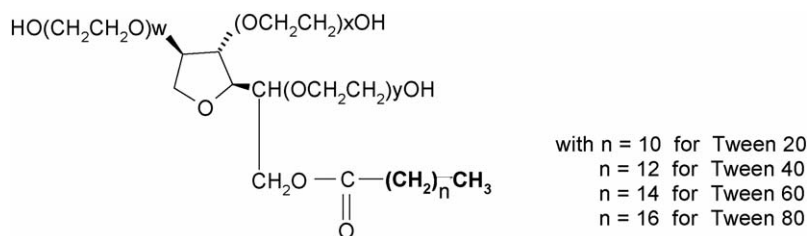


Fig. 3. Structure of Tween[®] molecules.

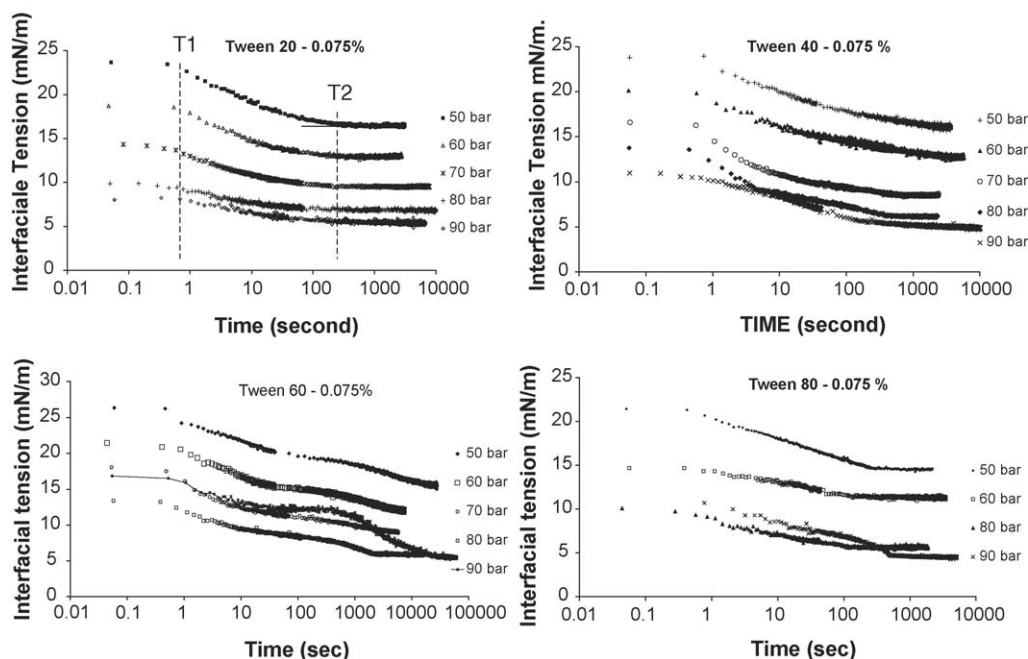


Fig. 4. Kinetics of γ decrease in presence of Tween[®] 20, 40, 60, and 80 at a bulk water concentration of 0.075%. The measurements were performed at pressures ranged from 50 to 90 bar and at a temperature of 40 °C.

3.1. Interfacial properties of Tween[®] adsorbed layer

3.1.1. Kinetics

Fig. 4 shows the γ kinetics obtained at a temperature of 40 °C in presence of the four types of Tween[®] molecules and for CO₂ pressures between 50 and 90 bar. For all studied CO₂ pressures, and for the studied Tween[®] molecules, the kinetics show two steps of adsorption having characteristic time T1 and T2. An equilibrium state was observed before 3000 s. For any given type of Tween[®], the time T1 is almost constant, whatever the CO₂ pressure. Therefore, this part of the kinetics is mostly controlled by a phenomenon occurring in the water phase, such as diffusion of Tween[®] molecules. In presence of Tween[®] molecules, the period necessary to reach an equilibrium state is at least 10 times shorter than the necessary time for the pure interface to be equilibrated [17]. Furthermore, compared to the pure H₂O–CO₂ system [1,17], the Tween[®] molecules decrease significantly the γ equilibrium values. At this aqueous concentration, almost of the Tween[®] molecules quickly reach the interface and inhibit the organization between the H₂O and CO₂ occurring for the clean interface [17].

These two steps kinetics are typical to them acquired for small surfactant molecules like Tween[®]. The first step can be attributed to the diffusion of the surfactant from the bulk aqueous phase to the “subsurface”, immediately adjacent to the interface. Then, the second step is attributed to the transfer of the molecules from the subsurface to the interface. For macromolecular surfactant, a third step can occur, due to interfacial rearrangements, involving reorientation, conformational changes, complex formation, chemical reactions, phase transitions, formation of three-dimensional structures resembling liquid crystals. . . For small molecules, rearrangement is generally a very fast process and has little effect on the overall behavior of adsorption.

Considering the curves obtained with Tween[®] 60, one obtained an irregular shape of the kinetic at a CO₂ pressure of 90 bar. Especially, the presence of four stages in the kinetic with a plateau at a value of 12 mN/m is remarkable. This phenomenon can be due to a competition effect between the adsorption of molecules of Tween[®] 60 and the organization that occurs between H₂O and CO₂ molecules under these conditions [17]. Similar observations were done for γ kinetics acquired in presence of aqueous ovalbumin concentration lower than 0.5 g/L [2]. This competition effect is not visible in presence of Tween[®] 20 and 40 molecules, perhaps because of their faster adsorption rate compared to Tween[®] 60. The smaller size of dodecyl and tetradecyl tails compared to hexadecyl alkyl chain, and the higher aqueous CMC values of Tween[®] 20 and 40 could explain this difference in the rate of adsorption. In presence of Tween[®] 80 molecules, a delay effect is visible on the γ kinetic measured for a CO₂ pressure of 90 bar, but this effect is less marked than for the Tween[®] 60 molecules. Therefore, the rate of surfactant adsorption at the H₂O–CO₂ interface is probably not the overall phenomenon that control the particular kinetic observed in presence of molecules of Tween[®] 60, but some sterical and thermodynamical consideration must be take into account, i.e. the molecules of Tween[®] 60 could promote the

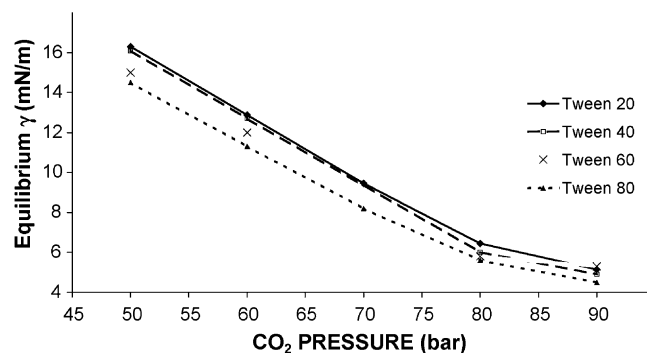


Fig. 5. Equilibrium γ vs. CO₂ pressure for the four types of Tween[®].

H₂O–CO₂ organization compared to the other type of Tween[®] molecules.

3.1.2. Equilibrium

For each types of Tween[®] molecules, the equilibrium γ decreases linearly with the CO₂ pressure in the range of 50–80 bar (Fig. 5). Then, in the range of 80–90 bar, the γ decrease is less pronounced. The shape of these curves versus the CO₂ pressure resemble the profile of γ measured at time 0 of the kinetics obtained at the pure interface (γ_0) [17]. The values of γ_0 are governed by the number of CO₂ molecules adsorbed at the interface interacting with H₂O molecules. From 80 bar, the water surface became saturated in H₂O–CO₂ complex, and γ_0 was then constant.

Except for the CO₂ pressure of 90 bar, the equilibrium γ decreases as the size of the alkyl chain increases. The more the Tween[®] molecules are hydrophobic, and the more their interfacial activity are great. This could be explained by their better partition between the two phases and by the higher degree of interaction between the CO₂ molecules and the alkyl surfactant tail. The equilibrium γ value observed at a CO₂ pressure of 90 bar in presence of Tween[®] 60 molecules, is however higher than the values obtained in presence of the other molecules. This could be explained by the formation of a mixed interface, composed of molecules of Tween[®] 60 and of a network made of organized H₂O–CO₂ molecules. This peculiar effect can be linked to the non-usual kinetic observed for Tween[®] 60.

3.1.3. Rheology

Fig. 6 compares the values of E_c (left) and E_{ne} (right) determined by the sinusoidal and ramp rheological approaches for the different types of Tween[®] and at various pressures. The low values of E_c are not slightly different according to the rheological method we used. At the contrary, the values of E_{ne} were influence by the kind of system and discrepancies are observed according to the method. However, E_c and E_{ne} values always change in the same way with the both approaches suggesting an experimental artefact. We can explain these differences by the fact that in the sinusoidal method, the value of E_{ne} is determined by extrapolation considering the position of the plateau in the $G'(\omega)$ curve (Eq. (13)), which in fact corresponds to the highest frequencies of the sinusoidal perturbations. From that there is in certain conditions, a skew on the determination of the posi-

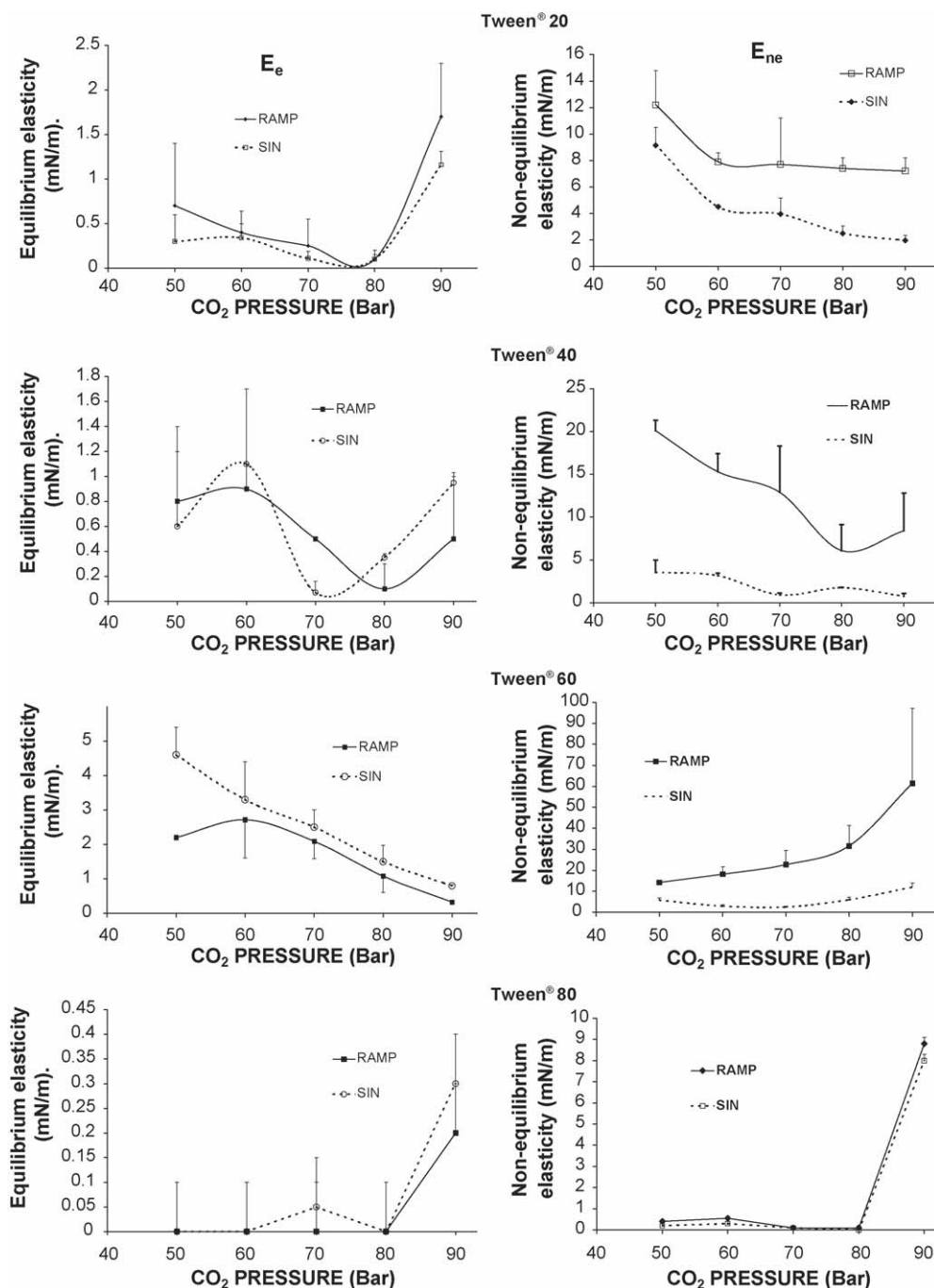


Fig. 6. Equilibrium and non-equilibrium interfacial elasticity determined by the both ramp and sinusoidal approach.

tion of the plateau and so on the value of E_{ne} . This experimental artifact can explain the almost constant difference between the two methods. From that we decided to compare the data using the ramp method.

For all the type of Tween® molecules except for Tween® 60, the values of E_e remain low from 50 to 80 bar, then increase a few for a pressure of 90 bar, indicating an increase of the interactions in the interfacial plane. For the Tween® 60 molecules, the E_e values always stay low with a tendency to decrease when the CO₂ pressure reach 90 bar, showing a decrease in the interactions in the interface. Furthermore, in same time that the E_e decreases,

E_{ne} increases, suggesting an increase of the interactions between the two phases and the interface.

Fig. 7 compares the equilibrium and non-equilibrium elasticities determined by the ramp approach for each type of Tween® molecules. The low equilibrium elasticities (E_e) of the interfacial layers formed with all Tween® molecules type and at all CO₂ pressures reveal weak interactions between the molecules at the interface. For CO₂ pressures between 50 and 80 bar, E_e and E_{ne} increase with the alkyl tail length until a maximal value obtained for 16 carbons. Then, E_e and E_{ne} decrease to values close to zero for an alkyl tail composed of 18 car-

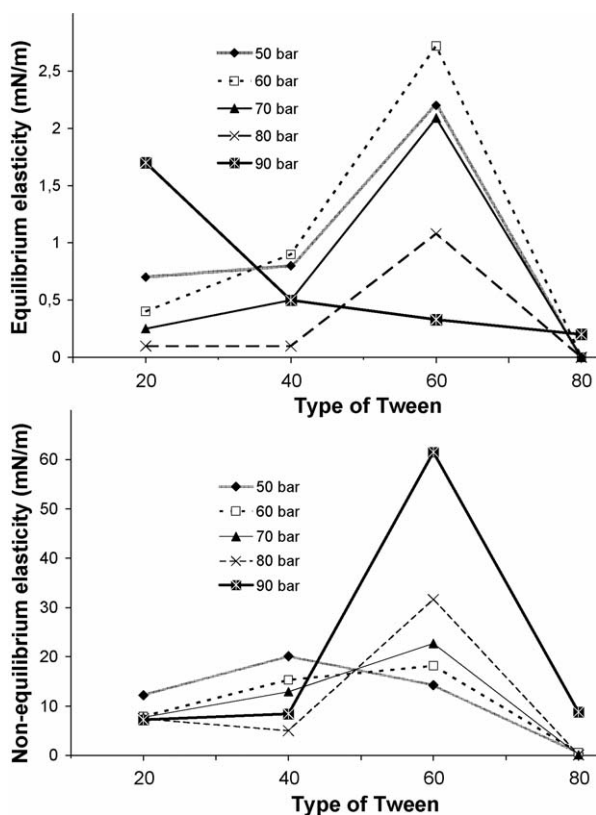


Fig. 7. Equilibrium and non-equilibrium elasticities vs. type of Tween[®] molecules determined by the ramp approach.

bons. This can suggest that the maximal interaction between the alkyl tails is developed when the tails are composed of 16 carbons. For a tail having a lower size, the aqueous solubilities of the Tween[®] molecules is high and the molecules are mainly in the aqueous phase. For a tail having more than 16 carbons, the aqueous solubility of the Tween[®] molecules becomes low, and the molecules are mainly directed into the CO₂ phase.

The results can suggest also that molecules of Tween[®] 60 are able to facilitate the organization between the H₂O and CO₂ molecules in order to form a mixed interfacial layer. This kind of structure could explain the great E_{ne} values observed at a CO₂ pressure of 90 bar, due to the great interactions between the Tween[®] molecules and the both phases.

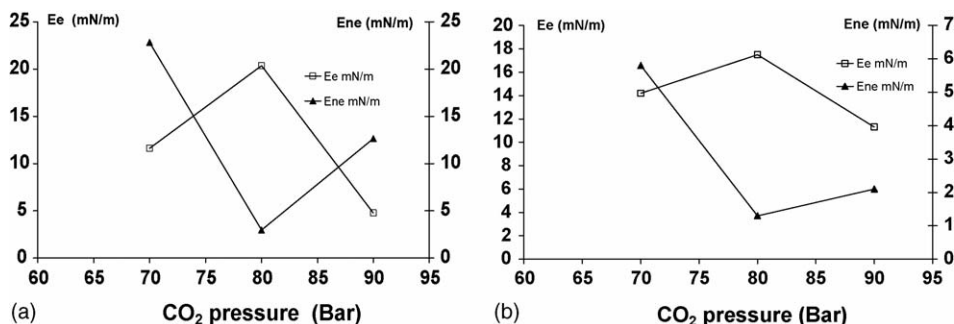


Fig. 9. HSA rheology. (a) Ramp type rheology and (b) sinusoidal type rheology.

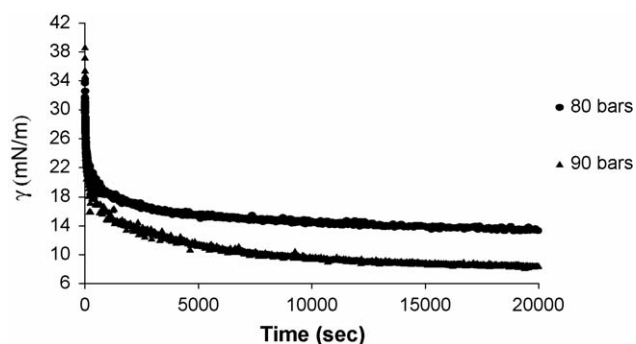


Fig. 8. Kinetics of HSA adsorption at water–CO₂ interface.

3.2. Interfacial properties of human serum albumin (HSA) adsorbed layer

3.2.1. Kinetics

Proteins are polymeric molecules made of the succession of 20 different possible monomers (amino acids) having various polarity. The parts or the segments of the protein composed in majority of apolar amino acids might form the more CO₂-phile segments of the protein. Fig. 8 presents the variation of γ versus time in presence of 0.84 g/L of a protein, the human serum albumin (HSA), at different pressures. The curves showed three steps to reach an equilibrium value, characterized by times of 40, 400 and 6000 s. This can be interpreted as a rapid adsorption of protein segments at the interface followed by a rearrangement of the adsorbed film that is frequently observed at water/oil interfaces [25]. In bulk solution, the less polar protein segments are in the heart of the protein, surrounded by the polar one. This organization is modified during the protein adsorption, leading to the three steps γ kinetics. At this aqueous concentration, the γ kinetic appears mainly controlled by the protein adsorption and not influenced by the interfacial organization of the H₂O and CO₂ molecules, like it is occurred in presence of ovalbumin (OVA) in this range of concentration [2].

3.2.2. Rheology

The rheological parameters have been determined in function of CO₂ pressure by the two approaches described above and similar results were obtained in both cases (Fig. 9). The comparison of both parameters E_e and E_{ne} indicated that the organization of the protein at the interface was influenced by the pressure and therefore by the density and polarity of CO₂. E_e reflects the den-

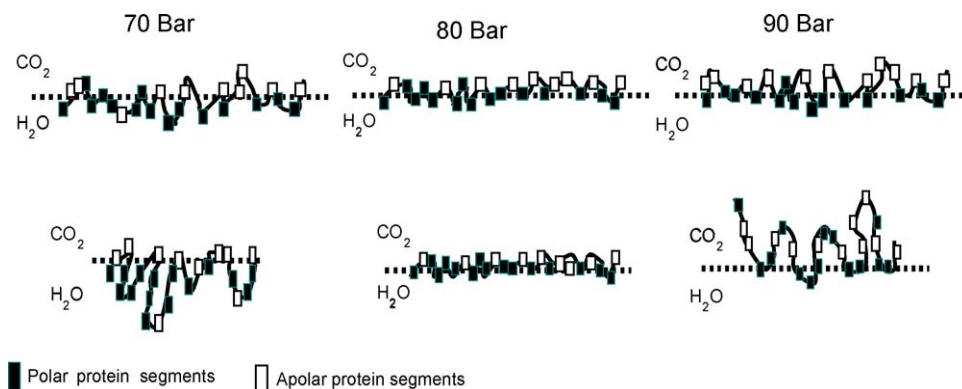


Fig. 10. Schematic representation of the HSA organization at the CO₂/H₂O interface at the three various pressures, before and after compression.

sity of segments anchored at the interface and their ability to stay in this conformation. In that way, E_e describes the lateral interaction between the segments of protein in the interfacial zone. E_{ne} characterizes the dissipation of the rheological perturbation energy related to interactions between some interfacial protein segments and bulk phases, the whole protein staying anchored at the interface due to the multiplicity of the fixed segments. These interactions occurs by the desorption of segments through the interface as loop-shape. One can see that E_e reached a maximum value near 80 bar, while E_{ne} gave a minimum value at this pressure. These results indicates that at a this peculiar pressure, the protein is strongly anchored at the interface and interacts similarly with both the adjacent phases (water and CO₂) (Fig. 10).

For a CO₂ pressure of 70 bar the dissipative characters of the interfacial layer is related to the expulsion of segments mainly towards the aqueous phase because of the low solvent power of the CO₂ for the most CO₂-phile protein segments (Fig. 10). At contrary we can assume that for 90 bar, the new dissipative characters of the interface can be linked to the expulsion of the most CO₂-phile protein segments, due to the energy bring by the interfacial compression, towards the CO₂ phase, which became a better solvent for these protein segments.

The difference of interfacial behavior observed between the HSA in this study and OVA in a previous one [2], can be linked to the difference between their amino acids sequences and between their initial spatial organizations. For example, the secondary structure of the OVA protein is composed of β sheets and helices [26], whereas HSA is only composed of helices [27].

As a matter of fact, for concentrations similar to those tested in this study, the OVA formed a strictly elastic interfacial layer with higher elasticity values than HSA, whatever the CO₂ pressure. HSA showed always a viscoelastic behavior with the conservative and dissipative contributions of the energy varying with the CO₂ pressure. Therefore, OVA might be more efficient for stabilizing the H₂O/CO₂ interface against the coalescence of water droplet dispersed in the CO₂ than the HSA.

On the other hand, the HSA and OVA proteins, at an initial aqueous concentration of 0.84 g/L, formed interfacial films having higher elasticity values than those obtained for all the Tween[®] molecules studied at an aqueous bulk concentration of 0.75 g/L. The difference in magnitude of E_e between the protein and the Tween[®] is probably related to the fact that lateral

interaction between protein segments forming rigid domains are important and cause a steric hindering in the film. At contrary, for small surfactant, lateral interactions involve Van der Waals attractive force and electrostatic repulsion which act between molecules and less between domains. On the other hand the small surfactants have a tendency to desorb upon compression (this is well indicated by the high values of E_{ne}). This desorption reduces the contribution of lateral interactions. Therefore, in these conditions, proteins seems more suitable to stabilize the H₂O/CO₂ interface against its breaking, which is a crucial factor in the coalescence of emulsion droplets.

4. Conclusion

We demonstrated that interfacial layers formed from classical and macromolecular amphiphiles can be analyzed by means of a pendant drop technique at the CO₂/H₂O interface. This technique allowed us to study the kinetics aspects of the adsorption and also to precisely measure the dilational properties of the films. Although the elasticity values measured by the two approaches are sometimes different, the way of variation is always similar. Even at high surfactant concentration, the organization of CO₂ with H₂O molecules can modify the kinetics of adsorption at the interface as well as their interfacial organization at the equilibrium.

Polymeric molecules like human serum albumin (HSA), produced interfacial films with an important elasticity. For these systems, E_e and E_{ne} varied with CO₂ pressure and can be controlled in order to stabilize W/C emulsion against the coalescence.

Those approaches are promising to better understand the phenomena that occur in the emulsion-based processes and indicate that a polymeric molecule could create a more cohesive film at the H₂O–CO₂ interface than little surfactant. Indeed macromolecules may be useful to inhibit the breaking of the CO₂–H₂O interfacial layer and thus the coalescence of water drop in a CO₂ surrounding media.

Acknowledgement

This work was financially supported by ADEME (Agence gouvernementale De l'Environnement et de la Maîtrise de l'Énergie), via the grant no. 0574C009.

References

- [1] F. Tewes, F. Boury, Formation and rheological properties of the supercritical CO₂–water pure interface, *J. Phys. Chem. B* 109 (2005) 3990–3997.
- [2] F. Tewes, F. Boury, Effect of H₂O–CO₂ organization on ovalbumin adsorption at the supercritical CO₂–water interface, *J. Phys. Chem. B* 109 (2005) 1874–1881.
- [3] Y. Ikushima, Supercritical fluids: an interesting medium for chemical and biochemical processes, *Adv. Colloid Interf. Sci.* 71–72 (1997) 259–280.
- [4] K. Sawada, M. Oshima, M. Sugimoto, M. Ueda, Microemulsions in supercritical CO₂ utilizing the polyethyleneglycol dialkylglycerol and their use for the solubilization of hydrophiles, *Dyes Pigments* 65 (2005) 67–74.
- [5] K. Harrison, J. Goveas, K.P. Johnston, E.A. O’Rear, Water-in-carbon dioxide microemulsions with a fluorocarbon–hydrocarbon hybrid surfactant, *Langmuir* 10 (1994) 3536–3541.
- [6] J. Eastoe, Z. Bayazit, S. Martel, D.C. Steytler, R.K. Heenan, Droplet structure in a water-in-CO₂ microemulsion, *Langmuir* 12 (1996) 1423–1424.
- [7] S.R.P. da Rocha, K.L. Harrison, K.P. Johnston, Effect of surfactants on the interfacial tension and emulsion formation between water and carbon dioxide, *Langmuir* 15 (1999) 419–428.
- [8] K.P. Johnston, Block copolymers as stabilizers in supercritical fluids, *Curr. Opin. Colloid Interf. Sci.* 5 (2000) 350–355.
- [9] B.H. Hutton, J.M. Perera, F. Grieser, G.W. Stevens, AOT reverse microemulsions in scCO₂—a further investigation, *Colloid Surf. A: Physicochem. Eng. Aspects* 189 (2001) 177–181.
- [10] J.L. Dickson, C. Ortiz-Estrada, J.F.J. Alvarado, H.S. Hwang, I.C. Sanchez, G. Luna-Barcenas, K.T. Lim, K.P. Johnston, Critical flocculation density of dilute water-in-CO₂ emulsions stabilized with block copolymers, *J. Colloid Interf. Sci.* 272 (2004) 444–456.
- [11] B.-S. Chun, G.T. Wilkinson, Interfacial tension in high-pressure carbon dioxide mixtures, *Ind. Eng. Chem. Res.* 34 (1995) 4371–4377.
- [12] D. Dittmar, R. Eggersa, H. Kahlb, S. Endersb, Measurement and modelling of the interfacial tension of triglyceride mixtures in contact with dense gases, *Chem. Eng. Sci.* 57 (2002) 355–363.
- [13] J.-Y. Park, J.S. Lim, C.H. Yoon, C.H. Lee, K. Pil Park, Effect of a fluorinated sodium bis(2-ethylhexyl) sulfosuccinate (aerosol-OT, AOT) analogue surfactant on the interfacial tension of CO₂ + water and CO₂ + Ni-plating solution in near- and supercritical CO₂, *J. Chem. Eng. Data* 50 (2005) 299–308.
- [14] J.L. Dickson, P.G. Smith Jr., V.V. Dhanuka, I. Srinivasan, M.T. Stone, P.J. Rosicky, J.A. Behles, J.S. Keiper, B. Xu, C. Johnson, J.M. DeSimone, K.P. Johnston, Interfacial properties of fluorocarbon and hydrocarbon phosphate surfactants at the water–CO₂ interface, *Ind. Eng. Chem. Res.* 44 (2005) 1370–1380.
- [15] D. Yang, P. Tontiwachwuthikul, Y. Gu, Interfacial interactions between reservoir brine and CO₂ at high pressures and elevated temperatures, *Energy Fuels* 19 (2005) 216–223.
- [16] P.A. Psathas, M.L. Janowiak, L.H. Garcia-Rubio, K.P. Johnston, Formation of carbon dioxide in water miniemulsions using the phase inversion temperature method, *Langmuir* 18 (2002) 3039–3046.
- [17] F. Tewes, F. Boury, Thermodynamic and dynamic interfacial properties of binary carbon dioxide–water systems, *J. Phys. Chem. B* 108 (2004) 2405–2412.
- [18] R. Ludwig, Water: from clusters to the bulk, *Angew. Chem. Int. Ed.* 40 (2001) 1808–1827.
- [19] Y.H. Mori, Clathrate hydrate formation at the interface between liquid CO₂ and water phases—a review of rival models characterizing “hydrate films”, *Energy Convers. Manage.* 39 (1998) 1537–1557.
- [20] T. Uchida, Physical property measurements on CO₂ clathrate hydrates. Review of crystallography, hydration number, and mechanical properties, *Waste Manage.* 17 (1997) 343–352.
- [21] P. Saulnier, F. Boury, A. Malzert, B. Heurtault, T. Ivanova, A. Cagna, I. Panaiotov, J.E. Proust, Rheological model for the study of dilational properties monolayers. Compartment of dipalmitoylphosphatidylcholine (DPPC) at the dichloromethane (DCM)/water interface under ramp or sinusoidal perturbations, *Langmuir* 17 (2001) 8104–8111.
- [22] F. Boury, T. Ivanova, I. Panaiotov, J.E. Proust, A. Bois, J. Richou, Dynamic properties of poly(DL-lactide) and polyvinyl alcohol monolayers at the air/water and dichloromethane/water interfaces, *J. Colloid Interf. Sci.* 169 (1995) 380–392.
- [23] A. Doisy, J.E. Proust, T. Ivanova, I. Panaiotov, J.L. Dubois, Phospholipid/drug interactions in liposomes studied by rheological properties of monolayers, *Langmuir* 12 (1996) 6098.
- [24] I. Panaiotov, T. Ivanova, J. Proust, F. Boury, B. Denizot, K. Keough, S. Taneva, Effect of hydrophobic protein SP-C on structure and dilatational properties of the model monolayers of pulmonary surfactant, *Colloids Surf. B: Biointerf.* 6 (1996) 243–260.
- [25] C.J. Beverung, C.J. Radke, H.W. Blanch, Protein adsorption at the oil–water interface: characterization of adsorption kinetics by dynamic interfacial tension measurements, *Biophys. Chem.* 81 (1999) 59–80.
- [26] P.E. Stein, A.G. Leslie, J.T. Finch, R.W. Carrell, Crystal structure of uncleaved ovalbumin at 1.95 Å resolution, *J. Mol. Biol.* 221 (1991) 941–959.
- [27] S. Lejon, I.M. Frick, L. Bjorck, M. Wikstrom, S. Svensson, Crystal structure and biological implications of a bacterial albumin binding module in complex with human serum albumin, *J. Biol. Chem.* 279 (2004) 42924–42928.